# Calculations of the electron-energy-loss spectra of silicon nanostructures and porous silicon

C. Delerue, M. Lannoo, and G. Allan
*Institut d'Electronique et de Microélectronique du Nord, Département Institut Supérieur d'Electronique du Nord, 41 Boulevard Vauban, 59046 Lille Cédex, France*
(Received 14 April 1997)

The electronic excitations in quantum-size silicon molecules, wires, or spheres are investigated by the evaluation of the full frequency-dependent dielectric matrix of the system. The calculation is based on a tight-binding framework in the random-phase approximation. The energy-loss spectra derived for fast electrons interacting with the nanostructures are dominated by collective excitations corresponding to bulk and surface modes even for nanostructures containing a small number of atoms. In contrast to the static screening, the dynamical properties are not strongly affected by the quantum confinement and are well described by the classical theories. We show that these collective modes are only slightly sensitive to surface defects and that low-energy excitations below 8 eV are only observable for one-dimensional silicon molecules, e.g., for polysilanes. These results are used to discuss the recent experimental observations made on fresh and oxidized porous silicon. [S0163-1829(97)03247-5]

The optical properties of semiconductor nanostructures are interesting both for fundamental physics and for applications. For example, the discovery of the visible light emission of porous silicon[1] has stimulated many studies in the field of artificial silicon nanostructures.[2] In spite of these efforts, there is not yet a consensus on the exact mechanisms of luminescence, in particular for small silicon and II-VI systems. The controversies come, in particular, from a lack of correlation between microscopic information such as the local crystallinity or the surface morphology and the optical properties. Therefore the atomic scale characterizations of the structure and chemistry are of particular interest. For example, the results obtained in the low-loss region (0–25 eV) by electron-energy-loss spectroscopy (EELS) using a scanning transmission electron microscope[3] (STEM) can relate spectroscopic information to structural ones. However their analysis is not direct and therefore requires detailed calculations of the EELS spectra to which one could compare. Several calculations of the EELS spectra of electrons moving on a definite trajectory past or through particles with various shapes have been published in the literature (see, for example, Refs. 4–6). The most sophisticated ones include all the multipole excitations but they are all based on the classical theory, describing the materials by their bulk local dielectric functions (these will be referred in the following as classical calculations). This is reasonable for large structures but it obviously fails to describe the systems in the molecular—or atomic—limit where the notion of collective excitations looses any value. In addition, the quantum confinement effects on the electronic structure which are not included in the classical theory may lead to drastic modifications of the screening properties as demonstrated recently in the static limit[7–9] where the average static dielectric constant of a semiconductor nanocrystal can be divided by a factor 2 compared to the bulk material. Finally, one must add that the classical calculations do not consider the influence of the surface or defect states which might be of growing importance for small particles.

Therefore our aim in this paper is to present a quantum calculation of the dynamic screening in silicon nanostructures. The dielectric matrix will be analyzed through the computation of the EELS spectra of electrons moving on a definite trajectory past or through silicon spheres, wires, or molecules, but of course the results are of more general interest since they can be applied to other dynamical properties of semiconductor nanostructures. For example, plasmons frequencies are of fundamental importance in the calculation of the quasiparticle spectra in the $GW$ formalism.[10] It is also of fundamental interest to see for very confined systems how the plasmons frequencies decrease to lower energies since basic principles show that plasmons frequencies should tend towards the interband transitions for one and two-dimensional systems in contrast to three-dimensional ones (see Ref. 11 for example). The paper is divided as follows. The calculation technique is described in the first paragraph as well as the macroscopic dielectric constant of bulk silicon. The calculated EELS spectra are presented in the second part for nanostructures perfectly passivated or with surface defects and for linear molecules. The last paragraph is devoted to the comparison with recent experiments made on porous silicon.

## I. BASIC THEORY

Unless otherwise stated, we consider throughout the paper silicon nanostructures passivated by hydrogen atoms like in Ref. 12. The calculation is divided into three distinct parts. First, the electronic structure of the nanostructure is computed to get the one-electron wave functions $u_k(\mathbf{x})$ of corresponding eigenvalue $\varepsilon_k$ [$\mathbf{x}=(\mathbf{r},\xi)$ where $\mathbf{r}$ is the position of the electron and $\xi$ is the spin variable]. For this we use a semiempirical tight-binding technique where the parameters of the Hamiltonian are adjusted to fit to the bulk silicon band structure and are transferred to the problem under consideration. This procedure is justified because the Hamiltonian inside the nanostructure is not expected to differ greatly from

 

the bulk silicon one. The silicon atoms are described by one $s$ and three $p$ orbitals and the hydrogen atoms by one $s$ orbital. We have chosen the Hamiltonian parameters of Ref. 13 because, when compared to other parametrizations, they give a good compromise between a reasonable bulk silicon band structure and a reasonable behavior of the bulk silicon dielectric function as discussed below. We have previously shown[14] that this parametrization[13] leads to an underestimation of the band-gap energy with the confinement which is due to a poor description of the conduction band in tight binding. However, this is not essential here since our study concerns spectra on a large energy range (0–25 eV) and that collective excitations do not depend too much on the details of the electronic structure. The interactions between silicon and hydrogen orbitals are taken from Harrison's rules.[15] The tight-binding technique is particularly suited to our problem because its computational simplicity allows studies from molecules to quite large systems (here typically 200 atoms). It is also a natural starting point to calculate the dielectric properties of a material.[16]

The second step of the calculation is the evaluation of the dielectric function of the system $\varepsilon(\mathbf{r},\mathbf{r}',\omega)$ for the response of the system to an external potential $V_{\text{ext}}(\mathbf{r},\omega)$ of frequency $\omega$,[10] which is done using the linearized time-dependent Hartree approximation often referred to as the random-phase approximation.[17,18,10] Then the dielectric function is related to the polarization function $P(\mathbf{r},\mathbf{r}',\omega)$:

$$\varepsilon(\mathbf{r},\mathbf{r}',\omega)=\delta(\mathbf{r},\mathbf{r}')-\int \nu(\mathbf{r},\mathbf{r}'')P(\mathbf{r}'',\mathbf{r}',\omega)d\mathbf{r}'', \quad (1)$$

where $\nu(\mathbf{r},\mathbf{r}')=e^2/|\mathbf{r}-\mathbf{r}'|$ and $P(\mathbf{r},\mathbf{r}',\omega)$ is given by

$$P(\mathbf{r},\mathbf{r}',\omega)=\sum_{kk'} \frac{n_k-n_{k'}}{\varepsilon_k-\varepsilon_{k'}-\omega-i\delta} f_{kk'}(\mathbf{r})f^*_{kk'}(\mathbf{r}'), \quad (2)$$

with $n_k$ is the occupancy of the state $k$ and

$$f_{kk'}(\mathbf{r})=\int u_k(\mathbf{x})u^*_{k'}(\mathbf{x})d\xi. \quad (3)$$

The full evaluation of $\varepsilon$ and $P$, for example, using the local-density approximation wave functions in a plane-wave basis is very demanding and even with the best computers it is generally restricted to systems with a small number of atoms.[19] As we use a description in an atomic localized basis and as the external potentials investigated here are slowly varying on the atomic scale, we dramatically simplify the equations by considering the functions as matrices in discrete values of $\mathbf{r}$ corresponding to the atomic positions $\mathbf{R}_i$. For example, the Eq. (1) transforms into a matrix equation:

$$\varepsilon=I-VP \quad (4)$$

if, considering the atomic volumes $\Omega_i$ and $\Omega_j$ located at $\mathbf{R}_i$ and $\mathbf{R}_j$, we define the elements of the matrices as (the dependence on the frequency being implicit):

$$P_{ij}=\int_{\mathbf{r}\in Q_i} P(\mathbf{r},\mathbf{r}',\omega)d\mathbf{r}d\mathbf{r}', \quad (5)$$

$$\varepsilon_{ij}=\int_{\mathbf{r}'\in Q_j}^{\mathbf{r}'\in\Omega_j} \varepsilon(\mathbf{R}_i,\mathbf{r}',\omega)d\mathbf{r}', \quad (6)$$

$$V_{ij}=\nu(\mathbf{R}_i,\mathbf{R}_j). \quad (7)$$

This formulation is a usual one in tight binding[20] and its main simplification is the neglect of the intra-atomic polarizations which is more justified for a covalent material like silicon.[20] However we have already shown[9] that it predicts a decrease of the static dielectric constant with size for small semiconductor systems in good agreement with other calculations.[7,8] It also gives a correct description of the screening at semiconductor interfaces.[21] The one-electron wave functions $u_k(\mathbf{x})$ are defined in the atomic basis $\{\varphi_{\alpha j}\}$ where $j$ denotes the atomic site at $\mathbf{R}_j$ and $\alpha \in\{s,p_x,p_y,p_z\}$:

$$u_k(\mathbf{x})=\sum_{j,\alpha} c_{kj\alpha}\varphi_{\alpha j}(\mathbf{x}). \quad (8)$$

Then, neglecting the overlaps between atomic wave functions, we rewrite the polarization:

$$P_{ij}=2\sum_{\substack{k\in VB\\ k'\in CB}} \left\{\sum_\alpha c_{k'j\alpha}c^*_{kj\alpha}\right\}\left\{\sum_\alpha c^*_{k'i\alpha}c_{ki\alpha}\right\} \times\left\{\frac{1}{\varepsilon_k-\varepsilon_{k'}-\omega-i\delta}-\frac{1}{\varepsilon_{k'}-\varepsilon_k-\omega-i\delta}\right\}, \quad (9)$$

where VB (CB) means the valence (conduction) band (without spin). The matrix of the Coulomb potential $V$ is defined as in our previous works:[9,22]

$$V_{ij}=e^2/|\mathbf{R}_j-\mathbf{R}_i| \quad \text{if } i\neq j,$$
$$V_{ii}=U \quad (10)$$

where $U$ is the intra-atomic Coulomb energy equal to 10.6 eV.[9,22] For systems having a translational periodicity like the bulk material or wires, the evaluation of Eq. (9) can be further simplified by using Fourier series (Appendix A). Then the matrices depend on a wave vector $\mathbf{q}$ but their size is given by the number of atoms in the unit cell.

To calculate the energy loss for fast electrons, we follow closely the procedure given by Ritchie,[23] valid for fast electrons.[10] Neglecting the electrodynamic retardation effects, the potential $V_{\text{ext}}(\mathbf{r},t)$ created by the electron along the axis $x$ with speed $\nu$ is obtained from the Poisson equation:

$$\Delta V_{\text{ext}}(\mathbf{r},t)=4\pi e\,\delta(x-\nu t), \quad (11)$$

which can be solved by Fourier transform:[23]

$$V_{\text{ext}}(\mathbf{k},\omega)=-\frac{8\pi^2 e}{k^2}\,\delta(k_x\nu+\omega). \quad (12)$$

Coming back to the real space, we get

$$V_{\text{ext}}(\mathbf{r},\omega)=-2\frac{e}{\nu}\exp\left(-i\frac{\omega}{\nu}x\right)K_0\left(\frac{\omega}{\nu}\sqrt{y^2+z^2}\right), \quad (13)$$

where $K_0$ is the modified Bessel function of order 0. For high-energy electrons (typically 200 keV), $V_{\text{ext}}$ is slowly variable on the length scale of the interatomic distance since $\omega/\nu\ll 1$ a.u. and it can be represented by a column matrix on the discretized space $[V_{\text{ext},i}=V_{\text{ext}}(\mathbf{R}_i,\omega)]$. The expression

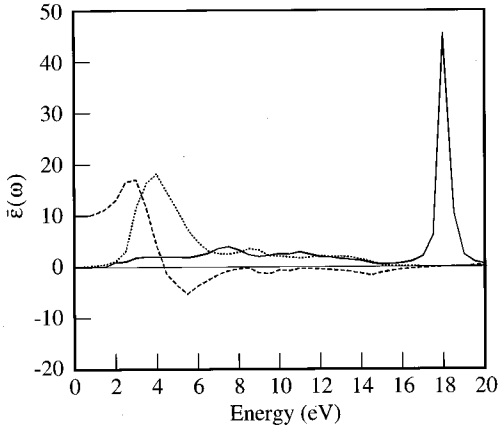


FIG. 1. Real (dashed line) and imaginary (dotted line) parts of the calculated macroscopic dielectric constant $\varepsilon(\omega)$ of bulk silicon. The full line corresponds to $\mathrm{Im}(1/\varepsilon(\omega))$.

of the energy loss $L(\omega)$ at a frequency $\omega$ is detailed in Appendix B and is given in the matrix formulation by

$$L(\omega) = -\frac{\omega}{\pi}\,\mathrm{Im}\{V_{\mathrm{ext}}^{\dagger}(-\omega)P(\omega)\varepsilon^{-1}(\omega)V_{\mathrm{ext}}(\omega)\}, \quad (14)$$

where $^{\dagger}$ defines the transposed matrix. Before discussing our results for the nanostructures, we need to look at the predictions of the model for the macroscopic dielectric constant $\varepsilon(\omega)$ of the bulk silicon for comparison. As usual and as defined in Appendix A, $\varepsilon(\omega)$ is given by the matrix elements of the inverse dielectric matrix for a vanishing small wave vector **q**. In Fig. 1 are plotted the real and imaginary parts of $\varepsilon(\omega)$, as well as $\mathrm{Im}(1/\varepsilon(\omega))$. Compared to experiments,[24] several points are satisfactory: the static dielectric constant of 9.8 (instead of 11.1), the presence of the main absorption band in the 3–6 eV range and the plasmon peak at $\sim$18.2 eV (instead of 16.9 eV). There are also some discrepancies. The optical spectrum $\mathrm{Im}(\varepsilon(\omega))$ around 4 eV is underestimated by about a factor 2 which is probably due to the neglect of the intra-atomic terms in the polarization but also to well-known problems inherent to the random-phase approximation[16] (excitonic effects could remove some of the disagreement[25]). There are also some spurious peaks in $\mathrm{Im}(\varepsilon(\omega))$ between 8 and 12 eV which are a consequence of the too flat conduction bands obtained in tight binding which gives marked peaks in the density of states (similar effects are obtained for diamond in Ref. 16). For a similar reason, the width of the plasmon peak in $\mathrm{Im}(1/\varepsilon(\omega))$ is too small because $\mathrm{Im}(\varepsilon(\omega))$ exactly vanishes above 16.3 eV, value which corresponds to the total width of the tight-binding band structure.[13] In principle, there should be electronic transitions from the valence band to the high-energy free-electron-like states which obviously are not included in a tight-binding treatment and which would give the correct behavior of $\mathrm{Im}(\varepsilon(\omega))$ at high energy.[26] Thus the width of the plasmon peak in Fig. 1 is only fixed by the arbitrary broadening $\delta$ in the polarization, Eq. (9) ($\delta = 0.2$ eV throughout the paper).

All these problems are the price to pay to get a simple formulation able to treat complex systems like nanocrystals. However, even if we do not expect fully detailed agreement with experiments, we believe that the trends in the physical effects induced by the confinement are correctly given as is the case for static properties.[9] For example, to emphasize these trends and for the sake of consistency, our results will be compared when possible to the best classical calculations,[4] where silicon will be described locally by the calculated dielectric function plotted in Fig. 1.

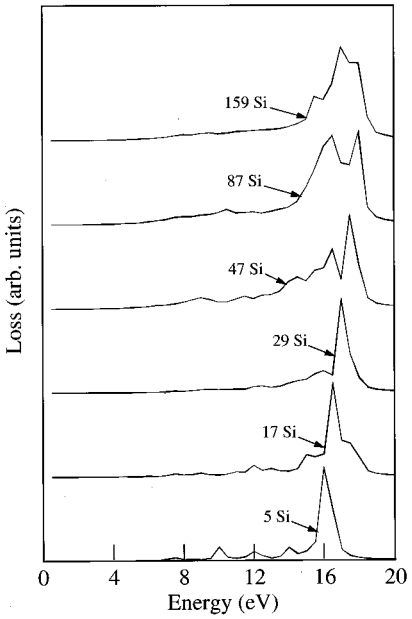


FIG. 2. Energy-loss spectra calculated for an electron probe (200 keV) passing through silicon spheres passivated by hydrogen ($b = 0$). The crystallites presented here are $Si_5H_{12}$ (diameter $d = 0.57$ nm), $Si_{17}H_{36}$ ($d = 0.86$ nm), $Si_{29}H_{36}$ ($d = 1.03$ nm), $Si_{47}H_{60}$ ($d = 1.21$ nm), $Si_{87}H_{76}$ ($d = 1.49$ nm), and $Si_{159}H_{124}$ ($d = 1.82$ nm).

## II. ENERGY LOSSES IN SILICON NANOSTRUCTURES

We first concentrate on silicon spheres with their surface completely passivated by hydrogen atoms. Figure 2 represents calculated loss spectra for a zero impact parameter $b$ ($b$ is the distance between the electron trajectory and the sphere center). The most interesting point is that even for very small nanocrystals, containing, for example, 17 silicon atoms, the spectrum is dominated by high-energy plasmon peaks above $\sim$11 eV and that the losses between 4 and 10 eV are quite low. This is particularly true for the larger systems containing 87 and 159 atoms (the differences between the two spectra come from different ponderations between the different plasmon modes[4]). This means that the damping via one-electron transitions does not appear even for very small structures simply because the collective excitations already occur at much higher energies than one-electron transitions. Figure 3 shows the loss spectra for the same spheres as Fig. 2 but for an impact parameter $b$ of 25 Å. The main difference with Fig. 2 is that the peak at higher energy disappears—at least for the biggest crystallites—which allows us to identify it as the ''bulk'' mode since we know it is not excited for an electron trajectory outside the sphere.[4,27] Thus the plasmon peaks obtained in Fig. 3 are surface modes.[27] In Fig. 3, we also plot the loss spectra calculated with the available classical theory[4] where, as explained in the previous section, the

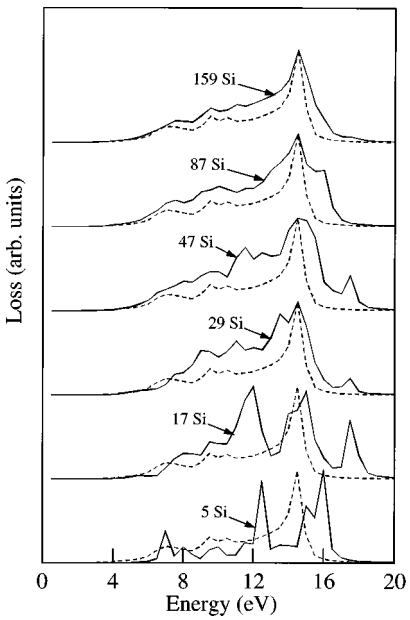


FIG. 3. Same as Fig. 2 but for an electron probe passing outside the spheres ($b=2.5$ nm) (straight line: full tight-binding calculation, dashed line: classical calculation).

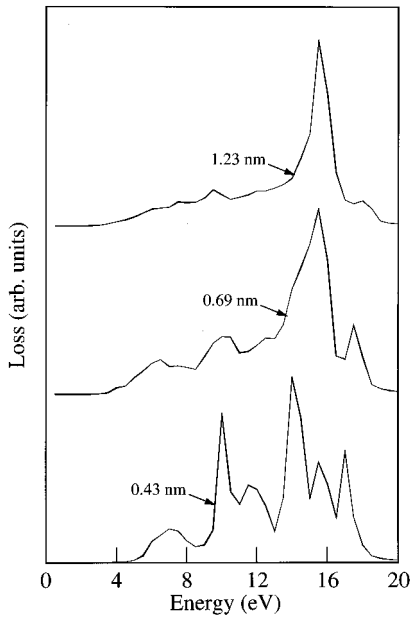


FIG. 4. Energy-loss spectra calculated for an electron probe (200 keV) passing through silicon wires ($b=0$) passivated by hydrogen for different diameters with a trajectory orthogonal to the axis of the wires.

local dielectric function of silicon is the calculated one plotted on Fig. 1. Comparing with the full calculation, we conclude that the classical theory is quite valid even for very small spherical nanostructures, e.g., containing 87 silicon atoms. A marked difference is obtained between the two calculations only for systems with less than $\sim 50$ atoms. We conclude that the confinement has a small influence on collective excitations of nanocrystallites while it has a dramatic one on the static dielectric constant. This is due to the fact that the static dielectric constant is quite sensitive to the near band-edge transitions—and thus to the band gap—while the plasmon frequencies which are at much higher energy than one-electron transitions are not very sensitive to details in the electronic structure (in first approximation, they are well defined by the average bonding-antibonding gap, see Appendix A).

Figure 4 shows the calculated loss spectra for cylindrical wires passivated by hydrogen. The situation considered here corresponds to a trajectory of the electrons orthogonal to the axis of the wire and passing through the center ($b=0$). As for the spheres (Fig. 2), the spectra are characterized by high-energy plasmon peaks corresponding to surface and bulk modes. The one-dimensional character of the system has not a dramatic effect on the plasmons because we know from the previous discussion that even for very small systems the modes are already characteristic of a three-dimensional system. Note that, to our knowledge, there is no classical analytical formulation of the losses for wires in the literature to which we could compare.

It is quite interesting to see how sensitive the plasmon peaks are to the presence of defects. In our particular case of silicon nanostructures, the stability of the Si-H bonds under focused irradiation by high-energy electrons can be questioned since the temperature of desorption of hydrogen is low ($\sim 250\,^{\circ}$C). In addition, the presence of dangling bonds is known to influence the luminescence properties of porous silicon.[12] Here we consider the extreme case where all the hydrogen atoms are removed and where the surface is not reconstructed. This leads us to a situation with the maximum number of dangling bonds giving a half-filled ''metallic'' band at the surface. By comparison with the fullerenes characterized by a half-filled $\pi$ band, we could expect some plasmon peaks at low energy ($\sim 6$ eV) induced by the presence of the band.[28] Figure 5 shows the loss spectrum for a sphere of $\sim 1.5$ nm with 87 silicon atoms and 76 dangling bonds at the surface ($b=0$) and for the passivated sphere for comparison. We see that the presence of the dangling-bond defects does not influence the spectrum too much in particular low-energy plasmons are not visible. The changes at high energy (14–19 eV) are partially due to electron transitions within Si-H states occurring in this range of energy. To understand the behavior at low energy, we have plotted on the same figure the loss spectrum calculated with the sums in the polarization $P$ [Eq. (9)] restricted to the dangling-bond states (filled for $k$ and empty for $k'$). Then we see the expected behavior with a low-energy plasmon peak at $\sim 3$ eV. However, the amplitude of this peak is very small compared to the others and the full spectrum is indeed dominated by the other high-energy modes of the sphere. Compared to the case of fullerenes, the essential difference is that the silicon clusters are filled by atoms and therefore three-dimensional characters are dominant.

One of the main conclusions of our work is that the collective excitations of the silicon nanostructures can be reasonably deduced from the dynamic screening properties of bulk silicon, with plasmons at quite high energy. Therefore different properties can only be expected for molecules. Here we present results for linear molecules (polysilanes) $H_3Si\text{-}(SiH_2)_n\text{-}SiH_3$ which can be seen as the extreme limit of thin wires (their electronic properties are discussed in Ref.

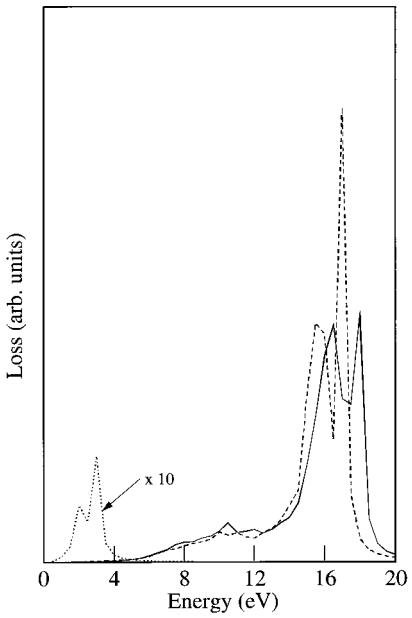


FIG. 5. Energy-loss spectra calculated for an electron probe (200 keV) passing through a silicon sphere containing 87 silicon atoms ($b=0$). The straight line corresponds to the passivated sphere $Si_{87}H_{76}$ ($d=1.49$ nm), the dashed line to the sphere with 76 dangling bonds at the surface. The dotted line is the spectrum calculated with the summations in the polarization restricted to the dangling-bond states [Eq. (9)].

29). The results of Fig. 6 correspond to an electron trajectory passing at one edge of the molecules and with an angle between the trajectory and the axis of the molecule of 45°. In contrast to previous results, and in particular to thicker wires (Fig. 4), the spectra are characterized by low-energy peaks, for example, between 6 and 8 eV lying in the region of one-electron transitions. However for such molecular systems, we expect that the large excitonic effects strongly influence the spectra,[29] for example, by shifting some peaks to lower energy [the exciton binding energy can be of the order of ~1 eV (Ref. 29)]. A more detailed analysis of these systems with a more complex theory including excitonic effects is planned.

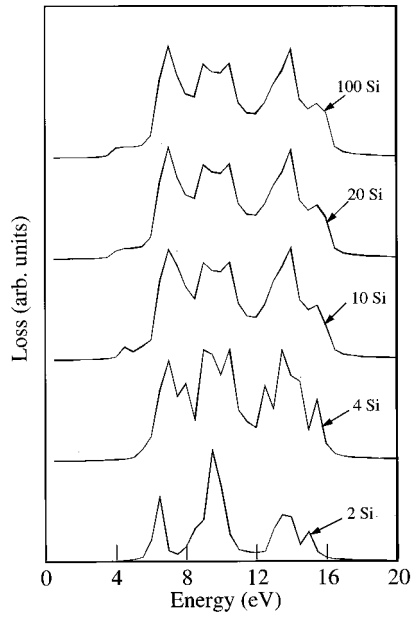


FIG. 6. Energy-loss spectra calculated for an electron probe (200 keV) passing at the edge of polysilanes $H_3Si\text{-}(SiH_2)_n\text{-}SiH_3$.

## III. COMPARISON WITH EELS ON POROUS SILICON

Porous silicon is an easy way to produce silicon nanostructures.[1] EELS studies on some porous *n*-type silicon samples[3] have clearly identified quantum-sized Si wires. The presence of oxygen was excluded which rules out the effect of some oxide layer on the results.[3] For a ~5-nm wire, the loss spectrum is dominated by a ~17.3-eV plasmon peak very close to the one of bulk silicon. As shown previously, this is quite expected since, already for much smaller nanostructures than those investigated experimentally, the loss spectra are dominated by ''bulk'' modes. A weak edge at 10.5 eV is also observed which can be interpreted by surface plasmons as demonstrated by our results or by the classical theory.[5] More surprisingly, a peak is obtained near ~4.5 eV with an intensity of magnitude similar to the other peaks. This was naturally interpreted[3] by the interband transitions which occur at the same energies.[12] This low-energy peak has been recently confirmed by another group[30] on hydrogenated porous *n*-type silicon where it has been proposed that the reduction of the static dielectric constant due to the confinement[7–9] could shift some plasmon peaks downwards to the observed value. Clearly both interpretations are not supported by our calculations which include the interband transitions and the effects of the confinement such as the reduction of the static dielectric constant. Even if the silicon structures observed experimentally are larger than the calculated ones, it is hard to imagine the appearance of a low-energy peak which would not exist for the smaller sizes calculated here or the larger ones where the classical theory becomes exact.

We have thus to examine other explanations for the ~4.5-eV peak. We have first studied the effect of the environment around the nanostructures by considering an ''effective medium'' with some dielectric constant typical of porous silicon or by considering a three-dimensional periodic array of crystallites simulating the porous medium: the results are quite close to those discussed above, without low-energy peaks. Second, we cannot completely exclude that effects going beyond the random-phase approximation may lead to an enhancement of the one-electron transitions: more sophisticated calculations, including in particular exchange and correlation effects in the response function, are necessary to conclude. Third, the low-energy peak may be due to some contaminants present in porous silicon. However, it seems that these contaminants are not detected experimentally.[3,30] Fourth, the peak could be due to the presence of silicon molecules in the pores like the polysilanes studied here since this is the only case for which we have obtained low-energy peaks. However, our calculated spectra (Fig. 6) show multiple peaks which are not visible experimentally[3,30] but, as discussed above, the excitonic effects may alter considerably the spectra. In addition, the presence of silicon molecules in the pores could explain the

strange behavior of the ~4.5-eV peak whose intensity does not decrease when moving the probe from the Si fibers into the vacuum.[3,31] However, one would still have to explain why on porous *p*-type silicon studied by STEM (Ref. 32) no peak is observed in the low-loss region while surface plasmons are clearly obtained in agreement with the theory.

## IV. CONCLUSION

We have shown that the energy-loss spectra of silicon nanostructures can be well represented by the classical theory, even for systems with a small number of atoms. The spectra are characterized by bulk and surface-plasmon modes with high energy. Theory at least within the random-phase approximation cannot explain the ~4.5-eV peak observed on porous *n*-type silicon, except possibly by the presence of silicon molecules in the pores which is the only case where low-energy excitations with substantial losses are predicted.

## ACKNOWLEDGMENTS

It is a pleasure to thank C. Lévy-Clément, C. Colliex, and N. Brun for fruitful discussions. The ''Institut d'Electronique et de Microélectronique du Nord'' is ''Unité Mixte 9929 du Centre National de la Recherche Scientifique.''

## APPENDIX A

For systems with translational symmetry, the atoms are located at the sites $\mathbf{R}_{jj_0}$, where $j_0$ is the index of the atom in the cell and $j$ is the index of the cell ($\mathbf{R}_j$). Then we can simplify the calculations by using Fourier series. For example,

$$\varepsilon_{i_0,j_0}(\mathbf{q})=\sum_j e^{i\mathbf{q}\cdot(\mathbf{R}_j-\mathbf{R}_i)}\varepsilon_{i_0 i,j_0 j}, \tag{A1}$$

which, by symmetry, does not depend on $i$. Then Eq. (4) transforms into

$$\varepsilon(\mathbf{q})=I-V(\mathbf{q})P(\mathbf{q}), \tag{A2}$$

where all terms are matrices with size equal to the number of atoms in the unit cell. The one-electron wave functions $u_{l,\mathbf{k}}(\mathbf{x})$ of energy $\varepsilon_l(\mathbf{k})$ belonging to band $l$ are built from tight-binding Bloch sums:

$$u_{l,\mathbf{k}}(\mathbf{x})=\frac{1}{\sqrt{N}}\sum_j e^{i\mathbf{k}\cdot\mathbf{R}_j}\sum_{j_0,\alpha} c_{j_0\alpha}(l,\mathbf{k})\varphi_{\alpha j_0 j}(\mathbf{x}), \tag{A3}$$

where $N$ is the number of atoms in the crystal. Then the polarization [Eq. (9)] is given by

$$P_{i_0,j_0}(\mathbf{q})=\frac{2}{N}\sum_{\mathbf{k}}\sum_{\substack{l\in VB\\ m\in CB}}\left\{\frac{\left(\sum_\alpha c^*_{i_0\alpha}(m,\mathbf{k})c_{i_0\alpha}(l,\mathbf{k}+\mathbf{q})\right)\left(\sum_\alpha c_{j_0\alpha}(m,\mathbf{k})c^*_{j_0\alpha}(l,\mathbf{k}+\mathbf{q})\right)}{\varepsilon_l(\mathbf{k}+\mathbf{q})-\varepsilon_m(\mathbf{k})-\omega-i\delta}\right.$$
$$\left.-\frac{\left(\sum_\alpha c_{i_0\alpha}(m,\mathbf{k})c^*_{i_0\alpha}(l,\mathbf{k}-\mathbf{q})\right)\left(\sum_\alpha c^*_{j_0\alpha}(m,\mathbf{k})c_{j_0\alpha}(l,\mathbf{k}-\mathbf{q})\right)}{\varepsilon_m(\mathbf{k})-\varepsilon_l(\mathbf{k}-\mathbf{q})-\omega-i\delta}\right\}, \tag{A4}$$

where the overlap terms have been neglected in the two-particle matrix elements consistently with the extreme tight-binding limit used here. To illustrate the problem, we can apply the formalism to bulk silicon in the molecular model. The system is roughly described by a set of $sp^3$ hybrid orbitals where only the resonance integrals $\beta$ between nearest-neighbor hybrids pointing towards each other are considered[20] ($\beta<0$). Then the matrix elements of the polarization are simply given in the real space by[20]

$$P_{i_0 i,i_0 i}=2/\beta_{\text{eff}},$$
$$P_{i_0 i,j_0 j}=-1/(2\beta_{\text{eff}}) \quad \text{if } i_0 i \text{ first neighbor of } j_0 j, \tag{A5}$$

where $1/\beta_{\text{eff}}=[1/(2\beta+\omega)]+[1/(2\beta-\omega)]$ if $\delta\to 0$. With two silicon atoms in the unit cell at (0,0,0) and ($a/4,a/4,a/4$) where $a$ is the lattice parameter, the polarization matrix is transformed in Fourier space into a $2\times 2$ matrix [given here for $\mathbf{q}=q(1,0,0)$]:

$$P(\mathbf{q})=\begin{bmatrix} 2/\beta_{\text{eff}} & -(1+e^{-iqa/2})/\beta_{\text{eff}} \\ -(1+e^{iqa/2})/\beta_{\text{eff}} & 2/\beta_{\text{eff}} \end{bmatrix}. \tag{A6}$$

The determination of the elements of the matrix $V(\mathbf{q})$ involves summations of the type

$$J=\sum_j \frac{e^{i\mathbf{q}\cdot\mathbf{R}_j}}{|\mathbf{R}_j-\mathbf{u}|}, \tag{A7}$$

which are evaluated numerically using the Ewald-Fuchs method[33,34] throughout the paper. In our particular case, the expressions in $V(\mathbf{q})$ can be approximated[20] and the full dielectric matrix is then derived from Eq. (A2). A quantity of practical interest is the macroscopic dielectric constant which describes the macroscopic response to a slowly variable perturbation.[35] Considering an external density of charge $\rho_{\text{ext}}(\mathbf{r})=e^{i\mathbf{q}\cdot\mathbf{r}}/V$ over the crystal volume $V$, we can calculate the $\mathbf{G}=\mathbf{0}$ component of the total charge as given by

$\int e^{-i\mathbf{q}\cdot\mathbf{r}}\rho_{\mathrm{tot}}(\mathbf{r})dV$. Using the Eqs. (5)–(7), we get the inverse of the macroscopic dielectric constant:

$$\overline{\epsilon(\omega)}^{-1}=\lim_{\mathbf{q}\to 0}\frac{1}{2}\sum_{i_0,j_0}e^{i\mathbf{q}\cdot(\mathbf{R}_{i_0}-\mathbf{R}_{j_0})}\varepsilon^{-1}_{j_0,i_0}(\mathbf{q}), \tag{A8}$$

which is given by the ratio of the $\mathbf{G}=\mathbf{0}$ component of the total charge to the same component of the external charge ($=1$ here). The fully calculated macroscopic dielectric constant is plotted in Fig. 1. In the case of the molecular model, the limit in Eq. (A8) can be obtained analytically:

$$\varepsilon(\omega)=1-\frac{2\pi}{\alpha\beta_{\mathrm{eff}}} \tag{A9}$$

Thus the static dielectric constant is $\overline{\epsilon(0)}=1-2\pi/a\beta$, which is equal to 5.16 with $\beta\approx -4$ eV.[13] It is much smaller than the experimental value due to the crude approximation of the polarization in the molecular model. The plasmon frequency $\omega_{\mathrm{pl}}$ is given by $\overline{\epsilon(\omega_{\mathrm{pl}})}=0$:

$$\omega_{\mathrm{pl}}=\sqrt{\frac{8\pi\beta}{a}+4\beta a^2}. \tag{A10}$$

We calculate $\omega_{\mathrm{pl}}=18.18$ eV which is very close to the value obtained by the full calculation (Fig. 1) showing that the plasmon frequency is much less sensitive to the details of the electronic structure than the static dielectric constant.

## APPENDIX B

We calculate here the energy loss of a fast electron interacting with some dielectric medium. The presence of the electron polarizes the medium. The variation of energy $d\Sigma$ of the medium during an infinitesimal time increment $dt$ can be written

$$d\Sigma=V^{\dagger}_{\mathrm{ext}}(t)d\rho_{\mathrm{ind}}, \tag{B1}$$

where $V_{\mathrm{ext}}$ is the column matrix ($V^{\dagger}_{\mathrm{ext}}$ a line matrix) of the potential created by the electron [given by the Eq. (13)] and $\rho_{\mathrm{ind}}$ is the column matrix of the induced charge in the medium. Transforming into frequency space, we have

$$V_{\mathrm{ext}}(t)=\frac{1}{2\pi}\int_{-\infty}^{\infty}e^{i\omega t-\alpha|t|}V_{\mathrm{ext}}(\omega)d\omega,$$
$$\rho_{\mathrm{ind}}(t)=\frac{1}{2\pi}\int_{-\infty}^{\infty}e^{i\omega t}\rho_{\mathrm{ind}}(\omega)d\omega, \tag{B2}$$

where $\alpha\to 0^{+}$ was added for convenience. The total variation of energy is given by $\int_{-\infty}^{\infty}d\Sigma$ which after integration on the time $t$—giving a $\delta$ function—becomes

$$\frac{i}{2\pi}\int_{-\infty}^{\infty}V_{\mathrm{ext}}(-\omega)\rho_{\mathrm{ind}}(\omega)\omega d\omega. \tag{B3}$$

Then, for finite systems like the spheres, the coefficients $c_{kj\alpha}$ are real, we have $P(-\omega)=P^{*}(\omega)$, $\varepsilon(-\omega)=\varepsilon^{*}(\omega)$ [Eq. (9)], and $V_{\mathrm{ext}}(-\omega)=V^{*}_{\mathrm{ext}}(\omega)$ [Eq. (13)]. Then the loss $L(\omega)$ at a frequency $\omega$ is given by

$$L(\omega)=-\frac{\omega}{\pi}\,\mathrm{Im}\{V^{\dagger}_{\mathrm{ext}}(-\omega)\rho_{\mathrm{ind}}(\omega)\}$$
$$=-\frac{\omega}{\pi}\,\mathrm{Im}\{V^{\dagger}_{\mathrm{ext}}(-\omega)P(\omega)\varepsilon^{-1}(\omega)V_{\mathrm{ext}}(\omega)\}. \tag{B4}$$

For systems with translational symmetry, the extension is straightforward:

$$L(\omega)=-\frac{\omega}{N\pi}\,\mathrm{Im}\sum_{\mathbf{q}}\{V^{\dagger}_{\mathrm{ext}}(-\omega,-\mathbf{q})P(\omega,\mathbf{q})$$
$$\times\varepsilon^{-1}(\omega,\mathbf{q})V_{\mathrm{ext}}(\omega,\mathbf{q})\}. \tag{B5}$$

The main advantage of the above formulation is that the evaluation of the dielectric matrix has only to be done within the volume of the dielectric material, and not in the vacuum. This is of practical interest in tight binding since the evaluation of the expressions (B4) or (B5) is a simple multiplication of finite matrices.


[1] L. T. Canham, Appl. Phys. Lett. **57**, 1046 (1990).
[2] W. L. Wilson, P. F. Szajowski, and L. E. Brus, Science **262**, 1242 (1993).
[3] A. Albu-Yaron, S. Bastide, D. Bouchet, N. Brun, C. Colliex, and C. Lévy-Clément, J. Phys. I (France) **4**, 1181 (1994).
[4] T. L. Ferrell and P. M. Echenique, Phys. Rev. Lett. **55**, 1526 (1985).
[5] R. Rojas, F. Claro, and R. Fuchs, Phys. Rev. B **37**, 6799 (1988).
[6] P. M. Echenique, J. Bausells, and A. Rivacoba, Phys. Rev. B **35**, 1521 (1987).
[7] R. Tsu and D. Babic, Appl. Phys. Lett. **64**, 1806 (1994).
[8] L.-W. Wang and A. Zunger, Phys. Rev. Lett. **73**, 1039 (1994).
[9] M. Lannoo, C. Delerue, and G. Allan, Phys. Rev. Lett. **74**, 3415 (1995); G. Allan, C. Delerue, M. Lannoo, and E. Martin, Phys. Rev. B **52**, 11 982 (1995).
[10] L. Hedin and S. Lundqvist, Solid State Phys. **23**, 1 (1969).
[11] Ben Yu-Kuang Hu and S. Das Sarma, Phys. Rev. B **48**, 5469 (1993).
[12] C. Delerue, G. Allan, and M. Lannoo, Phys. Rev. B **48**, 11 024 (1993).
[13] J. Van der Rest and P. Pêcheur, J. Phys. Chem. Solids **45**, 563 (1984).
[14] C. Delerue, G. Allan, and M. Lannoo, Phys. Rev. Lett. **76**, 2961 (1996).
[15] W. A. Harrison, Phys. Rev. B **24**, 5835 (1981).
[16] W. Hanke and L. J. Sham, Phys. Rev. Lett. **33**, 582 (1974).
[17] J. Lindhard, Dan. Math. Phys. Medd. **28**, 8 (1954).
[18] D. Pines, Solid State Phys. **1**, 367 (1955).
[19] G. Onida, L. Reining, R. W. Godby, R. Del Sole, and W. Andreoni, Phys. Rev. Lett. **75**, 818 (1995).
[20] M. Lannoo, Phys. Rev. B **10**, 2544 (1974).
[21] C. Priester, G. Allan, and M. Lannoo, Phys. Rev. B **38**, 9870 (1988).
[22] E. Martin, C. Delerue, G. Allan, and M. Lannoo, Phys. Rev. B **50**, 18 258 (1994).

[23] R. H. Ritchie, Phys. Rev. **106**, 874 (1957).
[24] Properties of Silicon, EMIS Datareviews Series No. 4 (INSPEC, London, UK, 1988), p. 72.
[25] M. del Castello-Mussot and L. J. Sham, Phys. Rev. B **31**, 2092 (1985).
[26] J. N. Decarpigny and M. Lannoo, Phys. Rev. B **14**, 538 (1976).
[27] Another way to identify the nature of the peaks is to plot the induced charge in the sphere.
[28] A. A. Lucas, L. Henrard, and Ph. Lambin, Phys. Rev. B **49**, 2888 (1994).
[29] G. Allan, C. Delerue, and M. Lannoo, Phys. Rev. B **48**, 7951 (1993).
[30] R. Masami Sassaki, F. Galembeck, and O. Teschke, Appl. Phys. Lett. **69**, 206 (1996).
[31] C. Colliex (private communication).
[32] I. Berbezier, J. M. Martin, C. Bernardi, and J. Derrien, Appl. Surf. Sci. **102**, 417 (1996).
[33] P. P. Ewald, Ann. Phys. (Leipzig) **64**, 253 (1921); Göttinger Nachrichten Math-Phys. KI. II **3**, 55 (1937).
[34] M. P. Tosi, *Solid State Physics: Advances in Research and Applications*, edited by F. Seitz and D. Turnbull (Academic, New York, 1964), Vol. 16, p. 107.
[35] S. L. Adler, Phys. Rev. **126**, 413 (1962); N. Wiser, *ibid.* **129**, 62 (1963).